Journal of Hazardous Materials 447 (2023) 130782

Contents lists available at ScienceDirect

Journal of Hazardous Materials

journal homepage: www.elsevier.com/locate/jhazmat

Research Article

Spatiotemporal evolution of U and Th isotopes in a mine effluent highly polluted by Acid Mine Drainage (AMD)

J.L. Guerrero [a,b,*], N. Suárez-Vaz [a], D.C. Paz-Gómez [a], S.M. Pérez-Moreno [a], J.P. Bolívar [a]

[a] Department of Integrated Sciences, Center on Natural Resources, Health and the Environment (RENSMA), University of Huelva, Campus El Carmen, 21071, Huelva, Spain

[b] Department of Earth Sciences, Center on Natural Resources, Health and the Environment (RENSMA), University of Huelva, Campus El Carmen, 21071, Huelva, Spain

HIGHLIGHTS

- Acid mine drainage comprises an important source of natural radionuclides.
- Conservative behaviour of U and Th isotopes in the mine effluent.
- Uranium is in the hexavalent state U(VI) in the form of uranyl sulphate complexes.
- Coprecipitation/adsorption of uranium with/onto Al-phases.
- Coprecipitation/adsorption of thorium with/onto Fe-oxyhydroxides.

GRAPHICAL ABSTRACT

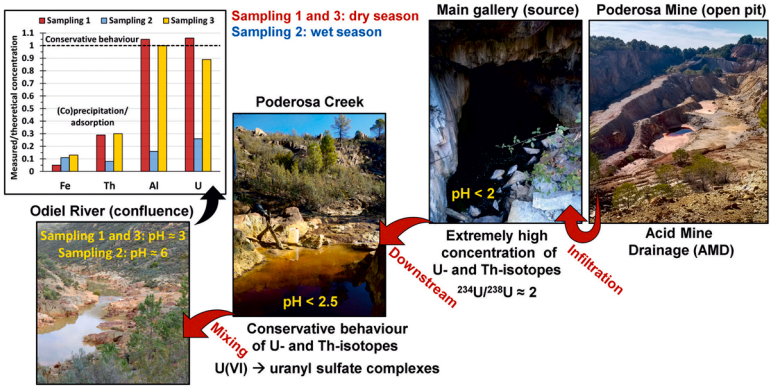

ARTICLE INFO

Editor: Edward Burton

Keywords:
U isotopes
Th isotopes
Acid mine drainage
Environmental impact
Conservative behavior

ABSTRACT

The spatiotemporal evolution of both U and Th isotopes in a mine effluent highly polluted by acid mine drainage (AMD) was evaluated. The acidic tributary, which born from the outflows of an abandoned sulfide mine, flows into the Odiel River. AMD comprises an important source of natural radionuclides, presenting concentrations of ^{238}U and ^{232}Th, two and four orders of magnitude higher, respectively, than the background values of surface continental waters. These natural radionuclides behave conservatively along the mine effluent (pH < 2.5) throughout the hydrological year. Under AMD conditions uranium is in the hexavalent state U(VI) and the main dissolved species are uranyl sulfate complexes. The polluted tributary has a significant impact on the Odiel River acidifying its waters during the low flow season and increasing up to one order of magnitude the activity concentrations of U and Th isotopes. U presented a conservative behavior in the Odiel River during the low flow season (pH ≈ 3), however it is removed from the liquid phase in the wet season (pH ≈ 6), probably due its coprecipitation/adsorption onto Al-phases. Th shows a high sensitivity to small increases of pH, and it is strongly coprecipitated/adsorbed with or onto Fe-oxyhydroxydizes in the river.

* Corresponding author at: Department of Earth Sciences, Center on Natural Resources, Health and the Environment (RENSMA), University of Huelva, Campus El Carmen, 21071, Huelva, Spain.

E-mail addresses: joseluis.guerrero@uhu.es (J.L. Guerrero), nuria.suarez@alu.uhu.es (N. Suárez-Vaz), daniela.paz@dci.uhu.es (D.C. Paz-Gómez), silvia.perez@dci.uhu.es (S.M. Pérez-Moreno), bolivar@uhu.es (J.P. Bolívar).

https://doi.org/10.1016/j.jhazmat.2023.130782
Received 28 November 2022; Received in revised form 4 January 2023; Accepted 10 January 2023
Available online 11 January 2023

1. Introduction

The exposure to water and oxygen of sulfide minerals, mainly pyrite (FeS_2), due to mining activities promote the formation of the so-called Acid Mine Drainage (AMD). Under weathering conditions, iron sulfide dissociates into sulfuric acid and ferrous ions that subsequently form ferric ions which can oxidize the sulfide minerals or precipitate as ferric hydroxide, generating the AMD [23,49]. This process generates acidic flows (pH = 2–3) with large concentrations of SO_4, Fe and accessory metals and metalloids (As, Cd, Co, Cu, Ni, Pb, Zn etc.) which have a significant source from other sulfides such as arsenopyrite (FeAsS), sphalerite (ZnS), chalcopyrite ($CuFeS_2$) or galena (PbS). On the other hand, these acidic leachates react with the host rock releasing elements such as Al, Ca, Mg, Mn, Si, etc. Mining activities involves the building of galleries, pits, and the stacking of tailings in spoil heaps which can store rainwater forming anthropogenic aquifers after the mine closure [1,22] acting as a source of AMD. The polluted outflows can severely damage the nearby environment acidifying and increasing the concentrations of pollutant metals and metalloids in the soils and groundwater/surface water [11,27,29,38], and AMD is indeed the main cause of polluted water at several locations worldwide.

The Iberian Pyrite Belt (IPB) located in the southwest of the Iberian Peninsula, is one of the largest metallogenic regions of massive sulfides in the world. The IPB extends from Spain in the east to Portugal in the west, with a length of over 200 km and a width around 40 km. The estimated massive sulfide reserves of this metallogenic province are above 1700 Mt [40]. The large-scale exploitation of these deposits took place during the 19th and 20th centuries [26], but mining works date from the year 2500 BCE. Pyrite with an amount over 90% of volume is the main sulfide mineral in the IPB but sphalerite, chalcopyrite and galena can also be found in variable amounts [40,50].

Along the IPB exist several old, abandoned mines without suitable reclamation measures acting as sources of AMD polluted leachates. The Odiel River, with 140 km length and a catchment area covering 2300 km^2, is the main water course draining the IPB. The upper river receives permanently these leachates which acidify its waters (pH ≈ 3) and increase the concentration of pollutant metals and metalloids [13,3,32,34,39]. In addition, it has been noticed that these acidic leachates present anomalous levels of natural radionuclides such as U and Th isotopes [15,17]. Due to the extreme physicochemical conditions of the Odiel River high concentrations of pollutants are transported in solution until reaching the estuary [15,17,18,3,32], where the neutralization of the acidic waters occurs producing its precipitation [15,17,51].

In natural environments, uranium is usually found in the oxidation states IV and VI. Under reducing conditions, uranium is predominantly in the tetravalent state, and tends to precipitate forming insoluble minerals; consequently, its concentration is extremely low. Otherwise, under oxidizing conditions uranium appears mainly as U(VI) in the form of the highly soluble uranyl ion UO_2^{2+}. The uranyl ions form complexes primarily with carbonate and phosphate under near-neutral conditions and with sulfate and fluorides at lower pH [37]. The mean activity concentration of ^{238}U in world rivers is around 6 mBq L^{-1}, [8,9]. The $^{234}U/^{238}U$ activity ratio (AR_U) in surface waters is generally higher than secular equilibrium ($AR_U = 1$) due to nuclide recoil during alpha-decay of ^{238}U and preferential dissolution of ^{234}U [16] showing a mean value in world rivers around 1.2 [8]. It is important to note that this ratio could be used to assess and monitoring the environmental impact of U isotopes due to industrial activities [20,21].

Thorium is found in nature only as a tetravalent cation. In contrast to uranium, which can be dissolved easily during weathering and transported as U(VI), thorium is a highly particle-reactive element and does not readily occur as a dissolved ion [25,52] being mainly transported by particles. Otherwise, in waters affected by AMD, due to the high acidity and sulfate concentrations, this radioelement tends to form soluble sulfate complexes such as $Th(SO_4)^{2+}$ and $Th(SO_4)_{2(aq)}$ [24]. The ^{232}Th activity concentration in world rivers show concentrations from 1 to 2 orders of magnitude lower than those of ^{238}U, usually showing the world rivers values below 0.1 mBq L^{-1} [8].

The levels and behavior of Naturally Occurring Radioactive Materials (NORM) in environments affected by uranium mining have been deeply studied [30,41,5–7], but in the case of metal mining such as Cu, Fe and Pb these have been traditionally overlooked and therefore a lack of knowledge exists. To study the behavior of natural radionuclides in AMD polluted aquatic systems, an abandoned mine from the IPB, called Poderosa Mine, was selected. The outflows from this sulfide mine generates a polluted tributary that flows into the Odiel River. In this work, U and Th isotopes activity concentrations were determined for different hydrological conditions in water samples collected at this hydrological setting.

The main objective of this study has been to analyse the spatiotemporal evolution and the behavior of both U and Th isotopes along a mine effluent highly polluted by AMD, from its source up to its confluence with the main river. The findings derived from this study can help to evaluate the potential radioactive impact of mine effluents into the nearby environment.

2. Study area

Poderosa Mine has 23 ha of affected surface and consists of two massive sulfide deposits (Fig. 1) mainly composed by pyrite with lesser amount of chalcopyrite, chalcocite and covellite, covered by a gossan layer. Despite its small size comprises a significant pollutant source in the Odiel River [14,4,44,47]. The north-west deposit is 175 m long and has an average thickness of 7 m while the deposit located in the south-east has around 150 m in length and 2 m thick, [4,36]. Mining was performed by combining surface exploitation and underground works generating a complex system of galleries and the stacking of large spoil heaps in the surroundings (Fig. 1). Around $6{\cdot}10^5$ t of sulfides were mined from 1864 to 1924, when due to the global fall in Cu prices the exploitation stopped. The open pit mining was restarted in the late 1980s to obtain Au and Ag from the south-eastern deposit by the exploitation of gossan, producing a new pit of around 1.9 ha. The old one located in the north-western deposit has a surface of around 1.1 ha and was filled with the overburdens removed from the new open pit. Some remediation measures were carried out during the 1990s, but the results were barely effective [42].

The polluted leachates generated in the underground system of Poderosa Mine are continuously released into the surface by a gallery, known as the main gallery, with an average flow around 1 L s^{-1} [4]. The outflows generate a creek about 600 m long, called Poderosa Creek, that flows into the Odiel River (see Fig. 1). A few meters from the gallery, Poderosa Creek joins with a channel that collects the acidic releases from the spoil heaps, and around 400 m downstream it joins a small stream, called El Soldado Creek, coming from another abandoned mine, El Soldado mine (Fig. 1).

3. Materials and methods

A sampling network with nine points was established. The location of these sampling points can be consulted in Fig. 1 and some pictures of them can be observed in Fig. 2. Five sampling points were located along Poderosa Creek (codes P1 to P5), from its source in the main gallery to its mouth, just before and after the confluence with the other streams. Another two points were in the channel that collects the outflows from the spoil heaps and El Soldado Creek, coded as C and S, respectively, just before the confluence with Poderosa Creek. Finally, another two sampling points were stablished in the Odiel River before and after the confluence with Poderosa Creek coded as O1 and O2, respectively. It is important to clarify that the location of the sampling points was selected to study the processes taking place where mixing of water occurs (P1 + C = P2, P3 + S = P4, P5 + O1 = O2).

At these points, water samples were collected under different

hydrological conditions: end of the dry season for two consecutive years (3/09/2018 and 2/09/2019) and wet season after heavy rains (7/11/2018). In Fig. S1 of the supplementary material the rainfall registered in the study area during the sampling period can be consulted.

In total, 27 water samples of 5 L each were collected in prewashed polyethylene bottles. Temperature, pH, electrical conductivity (EC) and oxidation-reduction potential (ORP) were measured *in situ* using a Crison MM40 + portable multimeter, with a 5048 (Ag/AgCl) electrode. The instruments were calibrated before sampling, and the ORP was corrected to obtain the redox potential in relation to the hydrogen electrode (Eh) according to Nordstrom and Wilde [33]. Water samples were filtered in the laboratory by using polycarbonate filters, 47 mm in diameter, with a pore size of 0.45 μm.

Two aliquots of each sample were taken for chemical analysis. A 100 mL aliquot for the analysis of dissolved elements, which was acidified up to pH < 2 to prevent adsorption processes onto the container walls with concentrated HNO_3 (65%) and an unaltered 50 mL aliquot for the analysis of SO_4. Major, minor and trace elements were determined by Inductively Coupled Plasma Optical Emission Spectroscopy (ICP-OES) and Inductively Coupled Plasma Mass Spectroscopy (ICP-MS) while the SO_4 concentration was determined by ion chromatography (IC) at Actlabs (Canada). Ion charges have been omitted in the tables and figures for simplicity. Actlabs is accredited to international standards as ISO/IEC 17025:2017 and ISO 9001:2015. The quality control (QC) was developed by the measurement of Certified Reference Materials (CRMs) as well as a duplicate and a blank every ten samples.

Natural radionuclide concentrations in the collected samples were determined by a sequential extraction technique based on the use of tributyl phosphate (TBP), and subsequent electrodeposition onto stainless- steel disc (U and Th isotopes). The radioactive sources were counted by α-particle spectrometry using ion-implanted silicon detectors, with a 25% absolute efficiency. The QC for α-particle measurements was conducted by participating in annual international proficiency tests (International Atomic Energy Agency [IAEA] and the Spanish Nuclear Safety Council [CSN]), and by measuring both a blank and CRMs (IAEA-434) every set of six samples [2].

Hydrogeochemical modelling of mineral saturation indices (SI) and uranium speciation was performed using the code PHREEQC version 3 [35]. All calculations employed the wateq4f.dat database, which is included with the program.

4. Results and discussion

4.1. Physicochemical parameters

To understand the spatiotemporal evolution of U and Th isotopes in the studied system it is important to know well the hydrochemistry of the waters, including the physicochemical parameters and the concentration of the main dissolved species.

The Fig. 3 displays the physicochemical parameters (pH, EC and Eh) measured during the three samplings (see also Table S1 of the supplementary material). As was commented in the introduction section, Poderosa Creek born from the outflows of the main gallery (point P1). The samples collected at this point presented extremely low pH values (pH < 2), high EC (around 10 mS cm^{-1}) and Eh (≈ 600 mV) for the three samplings. Downstream (points P2 to P5), after the confluence with the channel and El Soldado Creek, Poderosa Creek retained a high acidity (pH < 2.5) in all cases. On the other hand, the EC decreased (Fig. 3B), especially during the second sampling (wet season), reaching a minimum value about 2 mS cm^{-1} and the Eh slightly increased to values above 650 mV. Unpolluted stream waters of the Odiel River basin have a pH around 7, Eh around 400 mV and EC in the range from 100 to 500 μS cm^{-1} [47]. These values demonstrate the high polluting potential of this mine effluent. It is interesting to note that between points P2 and P3 and P4 and P5 the physicochemical parameters remain unaltered which seems to indicate that there are no significant inputs of water or relevant hydrochemical processes occurring between these couple of points.

The waters from the channel also showed a high acidity (pH ≈ 2.5) and EC values (ranging from 2.7 to 3.7 mS cm^{-1}). The Eh values (> 700 mV) were higher than those of the gallery, as expected since it is a surface stream. These values demonstrate the high pollutant load of the leachates from the spoil heaps. On the other hand, El Soldado Creek (S) had a pH above 4 and EC values below 0.5 mS cm^{-1} which indicate the significantly lower pollution of this small stream.

The sampling points from the Odiel River showed a higher variability. The point O1, located before the confluence with Poderosa

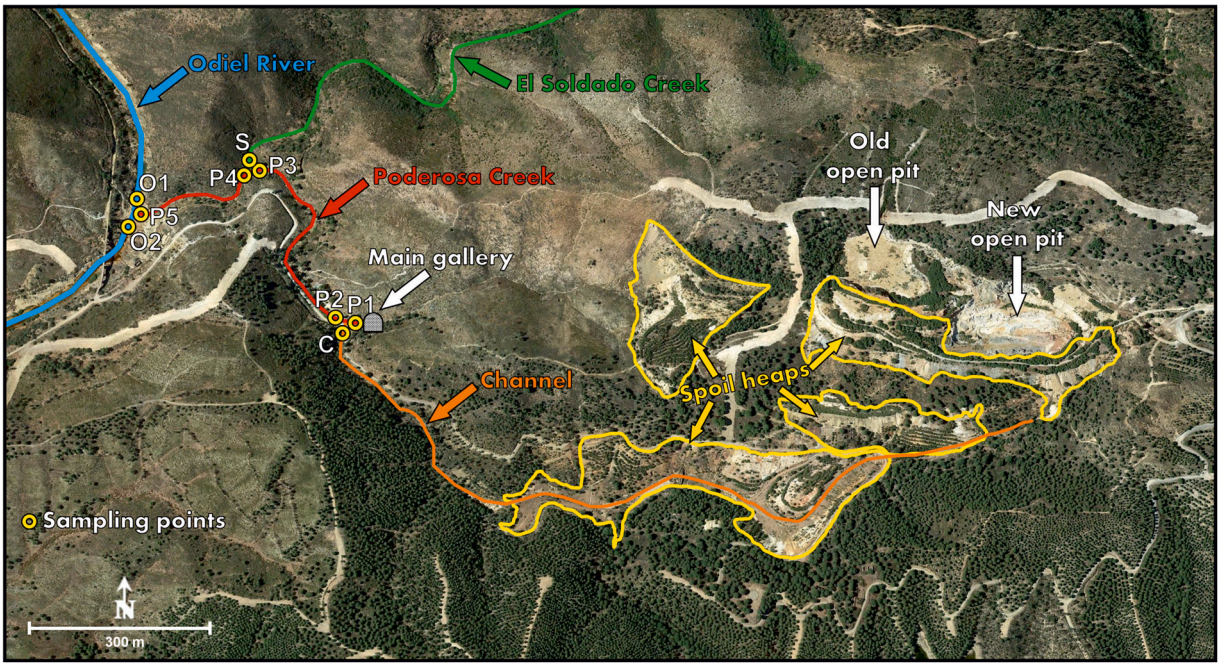

Fig. 1. Map of the study area showing the location of the sampling points. Different colours were selected to indicate the four main streams. P: Poderosa Creek; C: Channel; S: El Soldado Creek, O: Odiel River.

Creek, showed a pH above 6 for the first two samplings, indicating low AMD impact at this point, while for the third sampling the pH was around 4. The rainfall for the hydrological year 2017–2018 was 850 mm in the study area, slightly higher than the average value (740 mm) [12], while the hydrological year 2018–2019 was remarkably dry with a registered precipitation of 440 mm. The low flow of the Odiel River during the second year of study (sampling 3) explains its higher acidity. The EC at this point was lower than 1 mS cm^{-1} in the three samplings. After the confluence with Poderosa Creek (point O2), the Odiel River modified its physicochemical properties. In the first and third sampling (dry season), the pH decreased reaching values close to 3, while in the second sampling (wet season) remained above 6. Accordingly, the EC slightly increased in the river during the first and third samplings. The observed behavior demonstrates the natural attenuation that occurs in the Odiel River during the wet season and the acidification caused by Poderosa Creek during the low flow season.

4.2. Major elements

The Fig. 4 displays the concentrations of some of the major elements in the sampling points. SO_4, Fe and Al (Fig. 4A, B and C) are the main species in sulfide mine effluents and control the hydrochemistry of these polluted waters. The concentrations of all the major elements (11 in total) can be consulted in the Table S1 of the supplementary material.

The main gallery (point P1) showed high concentrations of SO_4 ($\approx 7{\cdot}10^3$ mg L^{-1}) and most of metals such as Fe $\approx 1.5{\cdot}10^3$ mg L^{-1}, Al $\approx 3{\cdot}10^2$ mg L^{-1} or Cu $\approx 1{\cdot}10^2$ mg L^{-1} as can be expected due to the AMD pollution of this system. The concentrations in the main gallery were very similar for the three samplings, which seems to indicate a low variability of the outflows from this mine aquifer over the hydrologic year. Furthermore, these concentrations are consistent with the obtained ones by Cánovas et al. [4], whose authors collected water samples in the gallery from December 2015 to November 2016. The concentration of sulfate and metals decreases downstream (points P2 to P5) from 40% to 60% for the first and third samplings (end of the dry season) and up to 90% in the second one (wet season) after the confluence with the channel and El Soldado Creek. To note that as in the case of the physicochemical parameters, between points P2 and P3 and P4 and P5 no variation was observed in the concentration of the studied elements, which confirm that there are no significant hydrochemical processes such as precipitation or redissolution at these sections.

In general, the channel (point C) showed notably lower concentrations of the studied elements than the groundwater from the gallery. For example, the concentrations of Fe and Al were two and one orders magnitude lower, respectively (Fig. 4A and B, Table S1). Otherwise, some elements such as Na, Ca and Mn had significantly higher concentration in the channel (Fig. 4E and F). It should be remembered that the channel collects the leachates from the spoil heaps and therefore the source of these elements is probably the acidic leaching of the host rock. A low hydrochemical variability was also observed at this point, but since the channel collects not only groundwater leachates from the spoil heaps but also runoff waters, a slight decrease in the concentrations can be observed in the second sampling during the rainy season. El Soldado Creek (point S) showed significantly lower concentrations than Poderosa Creek for most of the studied elements (Fig. 4, Table S1) due to its lower AMD pollution. In this creek, concentrations 1 order of magnitude lower of SO_4, 2 orders of magnitude lower of metals such as Al, Cu or Zn and up to 3 orders of magnitude lower of Fe (< 1 mg L^{-1}) were found.

The decrease in the concentrations of Poderosa Creek after the confluence with these two small streams (the channel and El Soldado Creek) could be explained by considering the percentage of water supplied from these affluents to the mix. These percentages were deter-

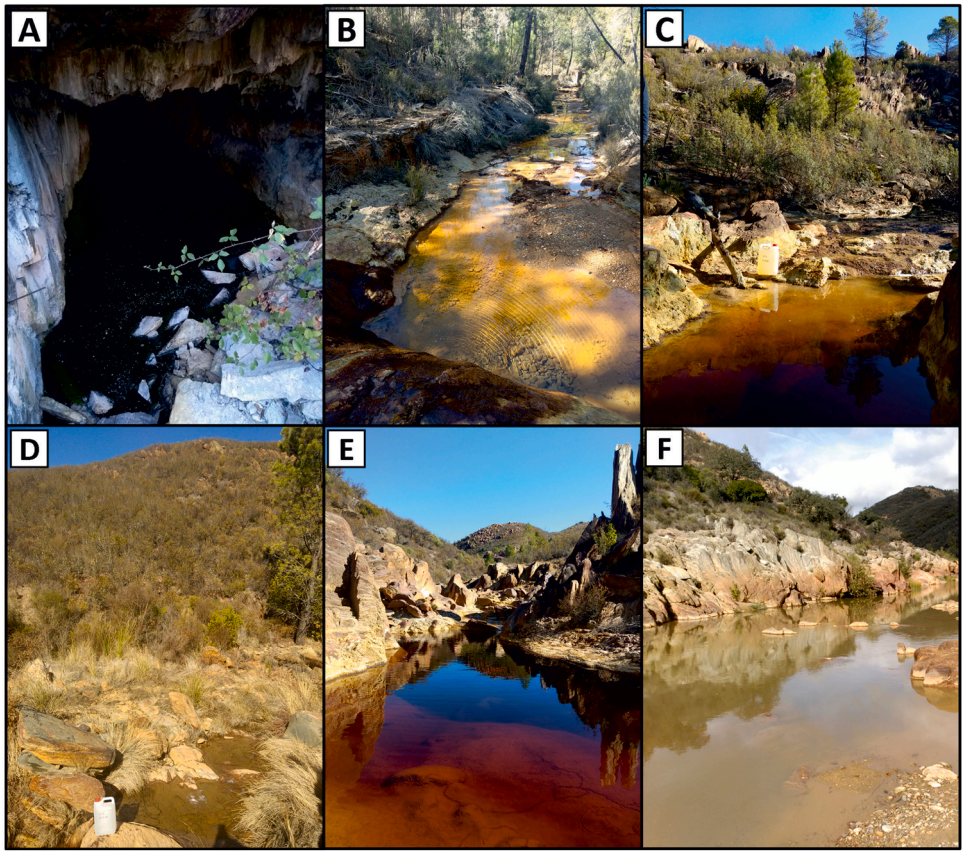

Fig. 2. Pictures of the sampling points. A: main gallery (P1); B: channel (C); C: Poderosa Creek (P3); D: El Soldado Creek (S); E: Poderosa Creek (P5); F: Odiel River (O1).

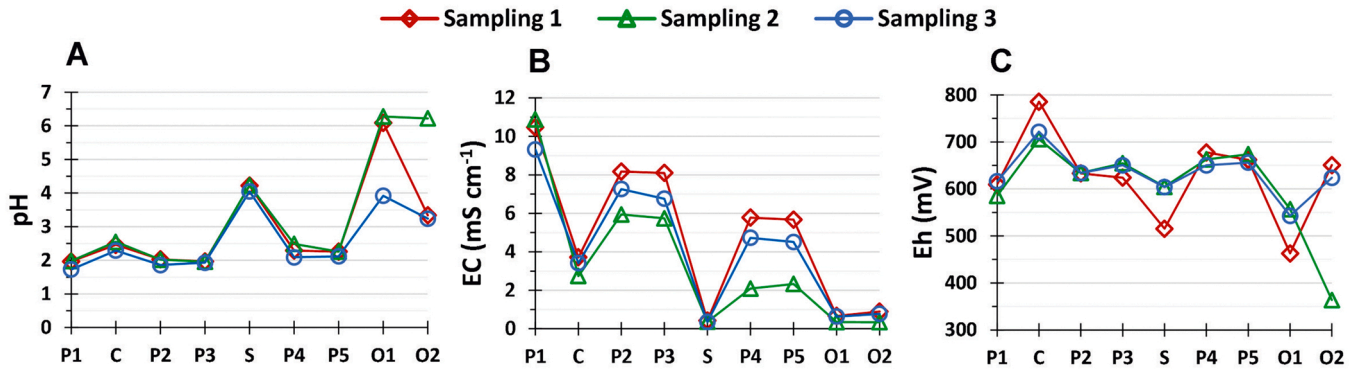

Fig. 3. Evolution of physicochemical parameters at the sampling points. First and third samplings: end of the dry season; second sampling: wet season.

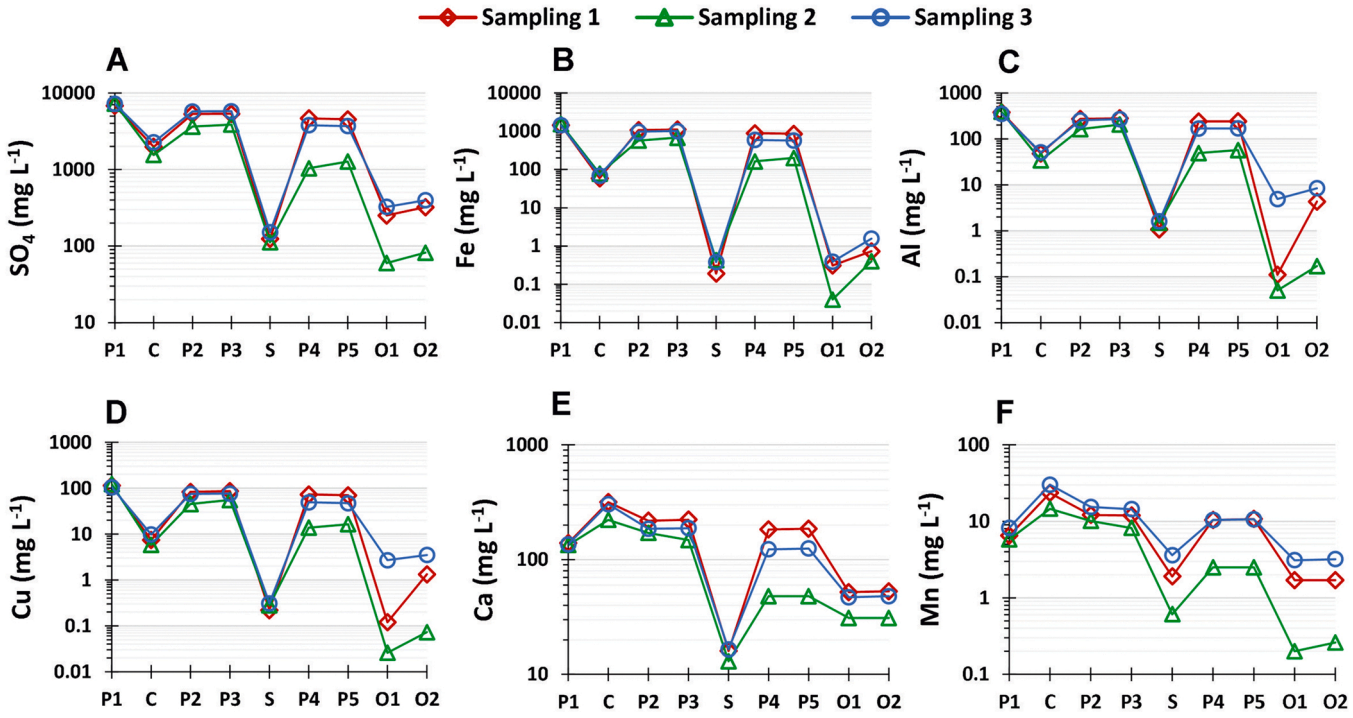

Fig. 4. Evolution of major elements at the sampling points. First and third samplings: end of the dry season; second sampling: wet season.

mined based on the conservative behavior of SO_4 under AMD conditions [10,28,38], as follows:

$$\text{Affluent water}(\%) = \frac{[X_{SO4}(PA)] - [X_{SO4}(PB)]}{[X_{SO4}(AF)] - [X_{SO4}(PB)]} \cdot 100 \quad (1)$$

where $[X_{SO4}(AF)]$ is the concentration of SO_4 in the affluent, and $[X_{SO4}(PB)]$ and $[X_{SO4}(PA)]$ are the concentrations of SO_4 at Poderosa Creek before and after the confluence, respectively.

The results showed that the percentage of water delivered by the channel to Poderosa Creek (point P2) was around 30% for the first and third sampling, but this percentage increased up to around 65% for the second sampling (wet season). On the other hand, the percentage of water supplied by El Soldado Creek to the mix was 13% and 35% for the first and third sampling respectively, while in the second one it increased up to 75%. These results could justify the different reductions in the concentrations of the studied elements for the wet/dry seasons after the mixing.

On the other hand, precipitation processes could also be involved in the decrease of the concentrations after the mixing, mainly for metals. While Fe tends to precipitate as Fe-oxyhydroxides in the form of jarosite ($pH \approx 2$) and mainly as schwertmannite (pH 2.5 – 4) for pH values lower than 4 or ferrihydrite ($pH > 5$), Al-phases as basaluminite or gibbsite needs pH values higher than 4–5 to precipitate [43,46]. The precipitation of Fe(III) and Al compounds can retain, by adsorption and/or coprecipitation processes some other metals and metalloids present in the polluted effluents by AMD. Therefore, iron and aluminum can act simultaneously on the one hand as strong buffering systems of the acidic solutions (at pH 2.5–3.5 and 4.5–5.0, respectively) and on the other hand as natural scavengers of trace elements.

A hydrochemical modelling of mineral saturation indices (SI) was performed with code PHREEQC. SI is an index where positive values identify potentially saturated minerals, while negative values identify potentially unsaturated minerals. The SI for the main iron and aluminum phases with positive values in the samples can be consulted in the Table S2 of the supplementary material. It was found that several iron phases such as hematite, jarosite, goethite, or magnetite present positive SI values along Poderosa Creek for the three samplings, reaching values up to around 6 in the case of hematite and k-jarosite in the final stretch after the confluence with El Soldado Creek (points P4 and P5). This fact indicates the potential precipitation of this saturated phases along the

creek. Otherwise, due to the low pH of Poderosa Creek the aluminum phases had negative values, which suggests that this element remains in the dissolved phase downstream.

The Odiel River showed concentrations several orders of magnitude lower than Poderosa Creek for most of the studied elements (Fig. 4, Table S1) before its confluence (point O1). It is remarkable the variability of the studied elements in that point led by the variability in the hydrochemical properties of the Odiel River (Fig. 3). The higher concentrations were found, as expected, during the dry season (first and third samplings) while in the second sampling, due to the larger flow, the previous washing of the riverbed and dilution by runoff, the concentrations of most studied elements were 1–2 orders of magnitude lower.

The flow of Poderosa Creek into the Odiel River (point O2) generates a significant increase in the concentrations of SO_4 and most of the studied metals (Fig. 4, Table S1), i.e., a great impact on the Odiel river waters. In the first sampling, the Odiel River increased one order of magnitude the concentrations of Al, and Cu, while Fe increased by 130% after the confluence. In the second sampling, despite the dilution by runoff, the concentration of Fe increased one order of magnitude in the Odiel River and metals like Al (200%) or Cu (180%) also significantly increased their concentrations. In the third sampling an important increase in the concentrations of Fe (300%) was observed in the Odiel River after the confluence. Moreover, the increase in the concentrations of Al (70%) and Cu (30%) was not as sharp as in the first sampling. The different behavior of these elements in the two samplings developed at the end of the dry season is explained by the different pH values of the Odiel River before and after the confluence as discussed in section 4.1.

By applying the Eq. 1 (considering Poderosa Creek as the affluent, and the Odiel River points before and after the confluence), the percentage of water supplied by Poderosa Creek into the mix was very low for the three samplings, around 2%, due to the small flow of this polluted stream in relation to the Odiel River. This percentage did not show significant variations during the hydrological year because the greater flow of Poderosa Creek after the rains is offset by the increase in the flow of the Odiel River.

The SI of the iron and aluminum phases in the Odiel River (Table S2 of the supplementary material) were also calculated. Before the confluence, several iron (such as goethite, hematite, magnetite or schwertmannite) and aluminum (such as $Al_4(OH)_{10}SO_4$, alunite, gibbsite, or diaspore) phases showed significant positive values (max. SI > 10) for the first and second samplings while in the third one the SI values of aluminum and some iron phases are negative as expected due to the lower pH value of the river. On the other hand, after the confluence with Poderosa Creek the SI values decreased for the samplings developed at the end of the dry season due to the acidification of the river and only some iron phases showed positive values. Otherwise in the second sampling since the pH of the river remained above 6 after the mix and the concentration of metals increased, the waters were strongly saturated of both iron and aluminum phases according to the SI obtained.

For a better understanding of the behavior of iron and aluminum in the studied system the theoretical concentrations of these elements in the mixing points (P2, P4 and O2) considering a conservative behavior were calculated as follows:

$$Xtheo = [X(AF)]\cdot AF + [X(MS)]\cdot MS \quad (2)$$

where [X(AF)] and [X(MS)] are the concentrations of the studied element (Fe or Al) in the affluent and the main stream before the mixing, while AF and MS are the parts per unit of water calculated from these streams in the mix (Eq. 1). Then, the behavior was evaluated by the ratio between the measured and theoretical concentrations. These ratios can be consulted in the Table S3 of the supplementary material. Values of this ratio around one indicates conservative behavior, while values significantly higher than one indicates an additional source of the radioelement in the mix (redissolution/desorption processes) and values significantly lower than 1 point out (co)precipitation/adsorption processes.

Despite the positive SI obtained of some iron phases, the sampling points located along Poderosa Creek (P2 and P4) showed values of this ratio above 0.90 for Fe which indicates a small removal of this element from the liquid phase after the confluence with the less polluted effluents (the channel and El Soldado Creek). The values obtained for Al (> 0.95) are in accordance with the negative SI observed for the aluminum phases, indicating a conservative behavior. On the other hand, the ratios calculated in the Odiel River after the confluence with Poderosa Creek demonstrate a strong removal of Fe from the liquid phase with values around 0.1 for the three samplings. Otherwise, Al only showed a clear precipitation during the second sampling in accordance with the SI for the aluminum phases, while during the dry season behaved conservatively.

4.3. Evolution of natural radionuclides

The Fig. 5 shows the evolution of ^{238}U and ^{232}Th activity concentrations and the $^{234}U/^{238}U$ and $^{230}Th/^{232}Th$ activity ratios at the sampling points. These values and the concentrations of U and Th by ICP-MS can be consulted in the Table S4 of the supplementary material. In the Fig. S2 the activity concentration of ^{238}U and ^{232}Th by α-spectrometry versus the concentration of U and Th by ICP-MS, respectively, were represented, obtaining a very good linear correlation with a coefficient of determination of 0.98 in both cases. Regarding the activity concentrations, the waters from the gallery had values about 700 mBq L^{-1} of ^{238}U, which is two orders of magnitude higher than the background values of world rivers [8,9]. The concentrations of ^{232}Th at this point ranged from about 200–300 mBq L^{-1}, three to four orders of magnitude higher than in surface continental waters [8]. The extremely low pH, high concentrations of SO_4 and additionally the high redox potential in the case of U, increase very significantly the mobility of U and Th isotopes under AMD conditions. Therefore, these high activity concentrations indicate the potential radioactive impact of this NORM effluent into the nearby environment. The $^{234}U/^{238}U$ ratio was very uniform around 1.7 at this point, showing a significant radioactive disequilibrium. Otherwise, the values for the $^{230}Th/^{232}Th$ ratio were close to 1.

The activity concentrations of ^{238}U and ^{232}Th in the channel were one and two orders of magnitude lower than in the main gallery, respectively, but higher than unperturbed waters due to the AMD pollution. To note that while in the gallery the concentrations of ^{238}U were from two to three times higher than those of ^{232}Th, at this point were from six to eight times higher probably due to the slightly higher pH that could favors its removal from the liquid phase. The studied activity ratios were slightly higher at this point, with values around 2 for the $^{234}U/^{238}U$ ratio and a maximum around 1.4 for the $^{230}Th/^{232}Th$ ratio. It should be considered that an intense chemical weathering favors lower $^{234}U/^{238}U$ activity ratios, since it is generated a fast uniform bulk mineral dissolution, which should not significantly fractionate ^{234}U from ^{238}U (Hussain and Krishnaswami,1980; Andersen et al., 2009). This fact seems to be the cause of the higher activity ratio in the samples from the channel, due to the more superficial leaching of the minerals from the spoil heaps. Accordingly, this ratio could be helpful to trace the source of polluted mine effluents. In addition, due to the higher AR_U of these polluted water regarding unperturbed surface water bodies ($^{234}U/^{238}U \approx 1.2$) this ratio could be also used to evaluate the radioactive impact by U isotopes into the aquatic systems due to the AMD.

In the samples from El Soldado Creek the concentrations of these natural radionuclides were below the detection limit by α-spectrometry (1 mBq L^{-1}), however according to the data of U and Th by ICP-MS (1 μg of U corresponds to 12.33 mBq of ^{238}U and 1 μg of Th corresponds to 4.05 mBq of ^{232}Th) the concentrations are 3 and 4 orders of magnitude lower, respectively, than in Poderosa Creek.

After the confluence with these two streams, the concentrations of the studied natural radionuclides in Poderosa Creek decreased

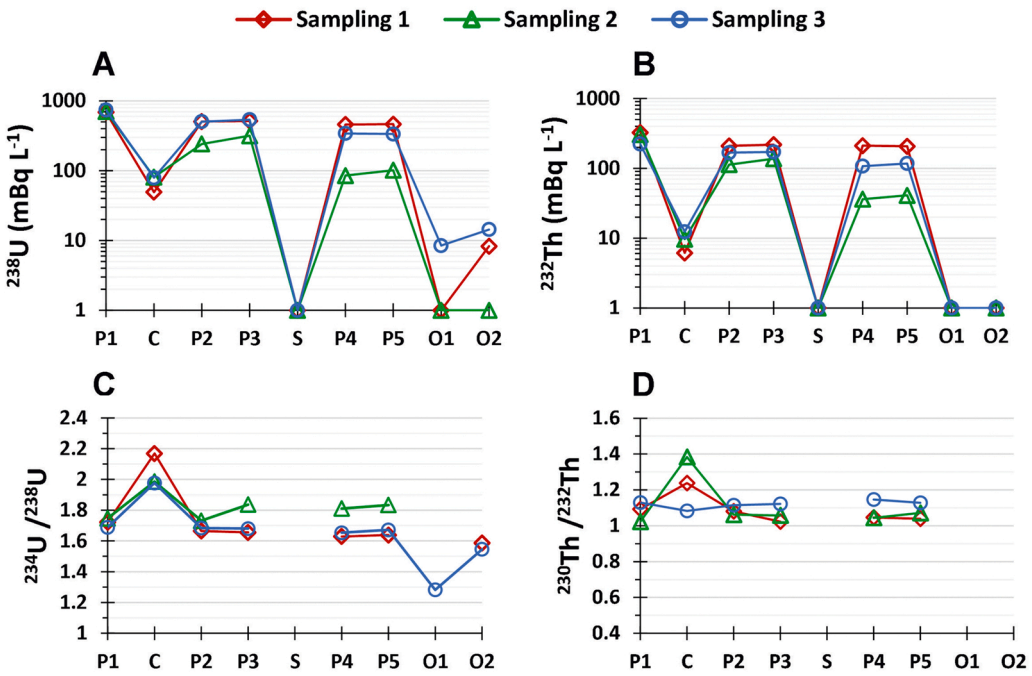

Fig. 5. Evolution of ^{238}U and ^{232}Th activity concentrations at the sampling points. First and third samplings: end of the dry season; second sampling: wet season.

downstream (point P5) from around 30–50% during the dry season (sampling 1 and 3), and up to a 90% in the wet season (sampling 2) similarly as was observed for the major elements. The $^{234}U/^{238}U$ ratio remained constant downstream in the sampling 1 and 3, while during the rainy season a slightly increase ($^{234}U/^{238}U \approx 1.8$) was observed due to the greater input of the channel. Otherwise, the $^{230}Th/^{232}Th$ ratio showed the same value along Poderosa Creek since the input of Th from the channel was negligible.

The activity concentration of ^{238}U in the Odiel River before the confluence with Poderosa Creek was below de detection limit (1 mBq L^{-1}) for the first and second sampling, while in the third sampling was around 8.5 ± 0.7 mBq L^{-1} with a $^{234}U/^{238}U$ ratio of 1.3. It should be remembered than the pH of the Odiel River at this point was around 6 during the samplings 1 and 2, while in the sampling 3 it was lower (pH < 4). It is well-known that U precipitates in the pH range from 4 to 6 [19,48], and it is redissolved due to the formation of carbonated complexes at higher pH values [15,17]. Therefore, our observations are in accordance with the behavior of U under environmental conditions. After the confluence, the activity concentration of this radionuclide in the Odiel River (point O2) increases for the first and third samplings (dry season), reaching values of 8.3 ± 0.6 and 14.4 ± 0.5 mBq L^{-1}, respectively. It should be noted the acidification of the Odiel River after the confluence during the dry season (pH ≈ 3). Otherwise, during the second sampling the activity concentration remain below the detection limit after the confluence. The $^{234}U/^{238}U$ ratio was around 1.5 at this point at the end of the dry season, slightly increasing due to the input of Poderosa Creek. This observation demonstrates the use of this ratio as a tracer of the radioactive pollution by ^{238}U-series radionuclides under AMD conditions.

Regarding the activity concentrations of ^{232}Th in the Odiel River, the values were below the detection limit for all the collected samples, both before and after the confluence with Poderosa Creek. However, the results by ICP-MS indicate that the concentrations of Th in the river increased one order of magnitude after the confluence with the polluted tributary.

To improve the understanding of U behavior and to evaluate the likely U mineral phases controlling solubility under AMD conditions, a hydrogeochemical modelling of U speciation and mineral SI was performed with code PHREEQC. Unfortunately, Th is not included in the database of this software and therefore its speciation and SI were not modelled. Nevertheless, as discussed in the introduction section, under the sulfuric acid conditions generated by AMD, Th is very mobile in the dissolved phase in the form of soluble sulfate complexes. Otherwise, this radioelement tends to be coprecipitated/adsorbed for pH > 3–4 since it is a highly particle-reactive element.

Redox potential plays an essential role controlling the mobility of U in the water. Uranium speciation modelling confirms that all uranium is in the hexavalent state U(VI), as would be expected because of the redox potential of the samples (Fig. 3). These values were higher than the redox potential of the reaction $UO_2^{2+} + 4\,H^+ + 2e^- \rightarrow U^{4+} + 2\,H_2O$, $Eh^0 = 330$ mV. Therefore, these positive redox potentials (oxidant waters) favor the presence of oxidized U forms, likely U(VI).

Fig. 6 displays the percentage of U species in the collected samples. In the waters from Poderosa Creek and the channel the main dissolved species were uranyl sulfate complexes (UO_2SO_4 and $UO_2(SO_4)_2^{-2}$) ranging from around 80–90% of the total dissolved species for the three samplings. In El Soldado Creek due to its lower AMD pollution the uranyl ion (UO_2^{-2}) showed percentages above 50%, but significant amounts of UO_2SO_4 were also observed. In the Odiel River before the confluence with Poderosa Creek were relevant the uranyl silicate complexes ($UO_2H_3SiO^{4+}$) with percentages from 30% to 60%, but also significant percentages of the uranyl ion and uranyl sulfate species were obtained in the samples. Finally, after the input of Poderosa Creek, uranyl sulfate complexes were the dominant species in the waters of the Odiel River reaching percentages around 60% in the three samplings. In addition, significant percentages of the uranyl ion (from around 30–40%) were obtained at this point.

The SI of the main U mineral phases are displayed as box plots (Fig. 7). The top and bottom of the box are the first quartile (Q1) and the third quartile (Q3), respectively, and the distance between them is the Interquartile Range (IQR). Data beyond the 1.5 • IQR may be considered as outliers (extreme values), extending the whiskers to the highest and lowest non-outliers.

As can be observed all samples were clearly undersaturated with respect to the studied U minerals: gummite (SI: −13 to – 5); schoepite (SI: −11 to −4); U_3O_8 (SI: −37 to −12); U_4O_9 (SI: −69 to −25); amorphous UO_2 (SI: −27 to −14); $UO_2(OH)_2(\beta)$ (SI: −10 to −3); UO_3 (SI: −13 to −5); uraninite (SI: −21 to −8). Therefore, it is not expected the

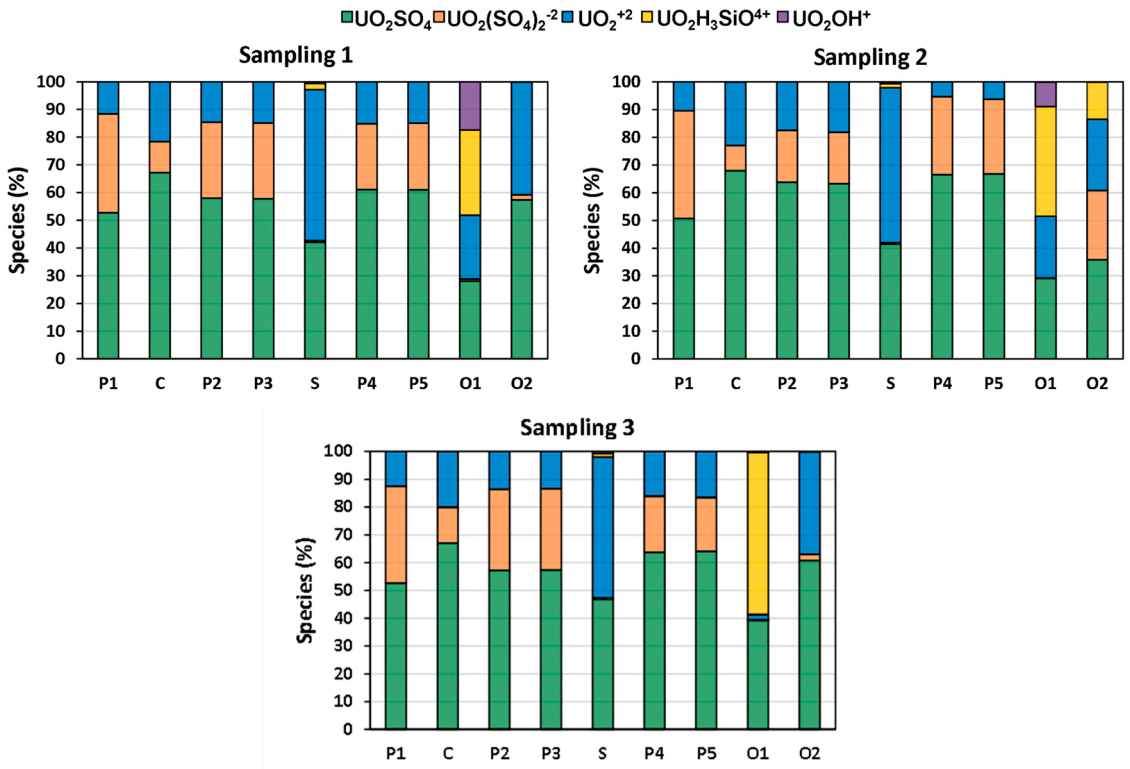

Fig. 6. Percentage of dissolved U species in the samples. First and third samplings: end of the dry season; second sampling: wet season.

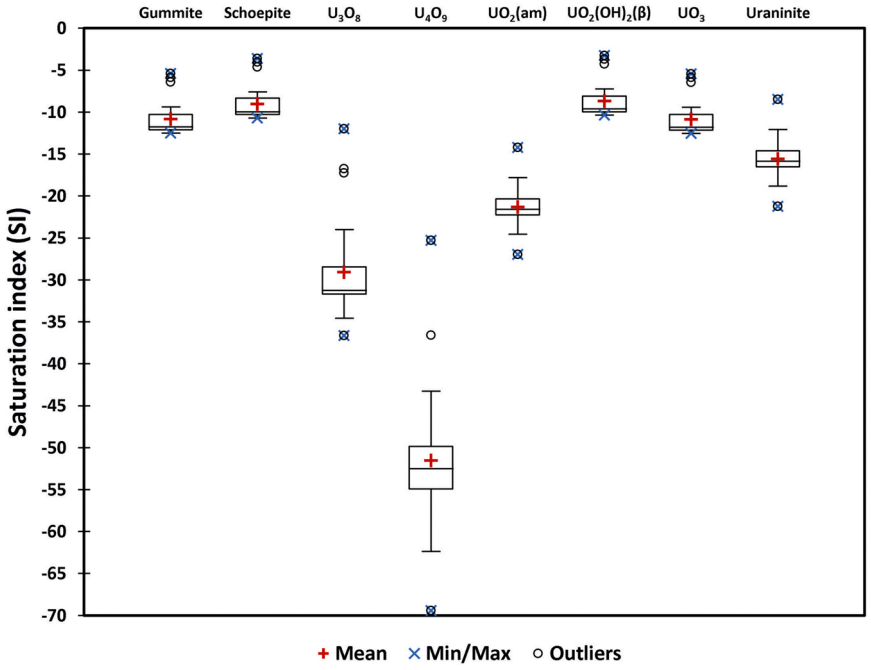

Fig. 7. Box plots of the SI obtained for the U mineral phases in the samples. Central line: median; box limits: first and third quartiles; whiskers: minimum and maximum non-outliers.

precipitation of U mineral phases under the studied AMD conditions.

However, both U and Th can be retained by adsorption and/or coprecipitation onto the iron and aluminum phases precipitating in the Odiel River after the confluence. To study this, the theoretical concentrations of these radioelements in the mixing points (P2, P4 and O2) considering a conservative behavior were calculated according to Eq. (2). Then, as in the case of iron and aluminum, the behavior was evaluated by the ratio between the measured and theoretical concentrations. These ratios can be consulted in the Table S5 of the supplementary material. The ratios were close to 1 for both U and Th isotopes along Poderosa Creek (points P2 and P4) indicating a conservative behavior of these radioelements in accordance with the low or no precipitation of Fe and Al-phases (Section 4.2). Otherwise, in the Odiel River (point O2) Th showed values around 0.3 for the samplings

developed at the end of the dry season and lower than 0.1 for the second sampling. These values indicate the coprecipitation/adsorption of Th with/onto the iron phases precipitating after the confluence of Poderosa Creek with the Odiel River. On the other hand, U only seems to be significantly removed from the liquid phase during the second sampling, which indicates that this radioelement tends to coprecipitate or to be adsorbed with/onto the aluminum phases that precipitate at the higher pH values (pH ≈ 6) reached in the river during the wet season.

The removal of U from the dissolved phase in this pH range is usually justified as coprecipitation with Fe-Mn hydroxides [17,31]. On the contrary, our data suggest that Al-phases have a key role in the coprecipitation/adsorption of U under AMD conditions. This finding was also documented by Sánchez-España et al. [45] in waters polluted by AMD from the IPB.

The observed behavior of Th and U in this study indicates that the Th transported in dissolution by highly acidic mine effluents as Poderosa Creek is mainly removed from the liquid phase when these polluted courses flow into the mainstream since a small increase in the pH provokes its coprecipitation/adsorption with/onto the iron phases. On the other hand, U needs higher pH values to be removed from the liquid phase probably due to coprecipitation/adsorption with/onto aluminum phases. These pH values are only reached during the wet season while during the dry season behaves conservatively along the watercourse being transported in dissolution to the estuary.

5. Conclusions

The behavior and spatiotemporal evolution of both U and Th isotopes in a mine effluent highly polluted by Acid Mine Drainage (AMD) was studied.

The conclusions obtained were as follows:

1. Acid mine drainage comprises an important source of natural radionuclides (U and Th isotopes) which have been traditionally overlooked. The ^{238}U and ^{232}Th activity concentrations are from two and four orders of magnitude higher, respectively, than the background values for surface continental waters, demonstrating the potential radioactive impact of these effluents into the nearby environment.
2. The $^{234}U/^{238}U$ activity ratio present significant radioactive disequilibrium in these polluted waters with maximum values around 2. This ratio could be used to evaluate the radioactive impact by U isotopes into the aquatic systems due to the AMD.
3. Poderosa Creek retains a very high acidity (pH < 2.5) throughout the hydrological year promoting a clear conservative behavior of the studied natural radionuclides. All samples were clearly undersaturated with respect to U mineral phases.
4. In the waters from the mine effluent uranium is in the hexavalent state U(VI) and the main U dissolved species are uranyl sulfate complexes (UO_2SO_4 and $UO_2(SO_4)_2^{-2}$). In the Odiel River after the confluence with Poderosa Creek uranyl sulfate complexes are also the dominant species in the waters reaching percentages around 60%.
5. Poderosa Creek has a significant and continued impact on the Odiel River acidifying its waters during the low flow season and increasing up to one order of magnitude the activity concentrations of U and Th isotopes.
6. Uranium presented a conservative behavior in the Odiel River after the confluence with Poderosa Creek during the low flow season (pH ≈ 3), but it is removed from the liquid phase during the wet season (pH ≈ 6), which indicates the coprecipitation/adsorption of this radioelement with or onto the Al-phases.
7. Thorium, a highly particle-reactive element, shows a high sensitivity to small increases of pH and it is strongly coprecipitated/adsorbed with or onto Fe-oxyhydroxides when the polluted effluent joins the main stem.

Funding

This research was funded by the University of Huelva and the Operative FEDER Program-Andalucía 2014–2020 (UHU-1255876, UHU-202020); The European Regional Development Fund through the Agencia Estatal de Investigación (research grant PID2020–116461RB-C21 and 116461RA-C22), and the Andalusian government (I+D+i-JAPAIDI-Retos project PY20_00096). José Luis Guerrero thank the Spanish Ministry of Universities for the Margarita Salas research grant. Funding for open access charge: Universidad de Huelva / CBUA.

CRediT authorship contribution statement

Category 1. Conception and design of study: J.P. Bolívar, J.L. Guerrero, D.C. Paz-Gómez. Acquisition of data: N. Suárez-Vaz, J.L. Guerrero, D.C. Paz-Gómez, S.M. Pérez-Moreno. Analysis and/or interpretation of data: N. Suárez-Vaz, J.L. Guerrero, J.P. Bolívar. Drafting the manuscript: J.L. Guerrero, S.M. Pérez-Moreno, D.C. Paz-Gómez. Revising the manuscript critically for important intellectual content: N. Suárez-Vaz, J.P. Bolívar, J.L. Guerrero, S.M. Pérez-Moreno. Approval of the version of the manuscript to be published (the names of all authors must be listed): J.L. Guerrero, N. Suárez-Vaz, D.C. Paz-Gómez, S.M. Pérez-Moreno, J. P. Bolívar.

Declaration of Competing Interest

The authors declare that they have no known competing financial interests or personal relationships that could have appeared to influence the work reported in this paper.

Data Availability

Data will be made available on request.

Acknowledgements

All persons who have made substantial contributions to the work reported in the manuscript (e.g., technical help, writing and editing assistance, general support), but who do not meet the criteria for authorship, are named in the Acknowledgements and have given us their written permission to be named. If we have not included an Acknowledgements, then that indicates that we have not received substantial contributions from non-authors.

Environmental Implication

Acid mine drainage (AMD) is the main cause of polluted water at several locations worldwide. Mine effluents from sulfide mines have a high acidity (pH = 2–3) and transport large concentrations of pollutants such as SO_4, Fe and accessory metals and metalloids abundant in this kind of deposits. In addition, AMD comprises an important source of natural radionuclides (U and Th isotopes) which have been traditionally overlooked. Uranium and thorium are hazardous radioelements and to study their levels, behavior and spatiotemporal evolution under AMD conditions is an essential tool to address their impact into the environment.

Appendix A. Supporting information

Supplementary data associated with this article can be found in the online version at doi:10.1016/j.jhazmat.2023.130782.

References

[1] Agboola, O., Babatunde, D.E., Isaac Fayomi, O.S., Sadiku, E.R., Popoola, P., Moropeng, L., Yahaya, A., Mamudu, O.A., 2020. A review on the impact of mining

operation: monitoring, assessment and management. Result Eng, 100181. https://doi.org/10.1016/j.rineng.2020.100181.
[2] Bolívar, J.P., Martín, J.E., García-Tenorio, R., Pérez-Moreno, J.P., Mas, J.L., 2009. Behaviour and fluxes of natural radionuclides in the production process of a phosphoric acid plant. Appl Radiat Isot 67, 345–356. https://doi.org/10.1016/j.apradiso.2008.10.012.
[3] Cánovas, C.R., Olías, M., Nieto, J.M., Sarmiento, A.M. y, Cerón, J.C., 2007. Hydrogeochemical characteristics of the Tinto and Odiel rivers (SW Spain). Factors controlling metal contents. Sci Total Environ 373, 363–382. https://doi.org/10.1016/j.scitotenv.2006.11.022.
[4] Cánovas, C.R., Macías, F., Olías, M., 2018. Hydrogeochemical behavior of an anthropogenic mine aquifer: implications for potential remediation measures. Sci Total Environ 636, 85–93. https://doi.org/10.1016/j.scitotenv.2018.04.270.
[5] Carvalho, F.P., Oliveira, J.M., Madruga, M.J., Lopes, I., Libanio, A., Machado, L., 2006. Contamination of hydrographical basins in uranium mining areas of Portugal. In: Merkel, B.J., Hasche-Berger, A. (Eds.), Uranium in the Environment: Mining Impacts and Consequences. Springer-Verlag, Berlin, Heidelberg, pp. 691–702. https://doi.org/10.1007/3-540-28367-6_70.
[6] Carvalho, F.P., Oliveira, J.M., Faria, I., 2009. Alpha emitting radionuclides in drainage from Quinta do Bispo and Cunha Baixa uranium mines (Portugal) and associated radiotoxicological risk. Bull Environ Contam Toxicol 83, 668. https://doi.org/10.1007/s00128-009-9808-3.
[7] Carvalho, F.P., Oliveira, J.M., Malta, M., 2011. Radionuclides in plants growing on sludge and water from uranium mine water treatment. Ecol Eng 37, 1058–1063. https://doi.org/10.1016/j.ecoleng.2010.07.011.
[8] Chabaux, F., Riotte, J., Dequincey, O., 2003. U-Th-Ra fractionation during weathering and river transport. Rev Mineral Geochem 52, 533–576. https://doi.org/10.2113/0520533.
[9] De Vos, W., Tarvainen, T., 2006. The Geochemical Atlas of Europe Part 2. Interpretation of Geochemical Maps, Additional Tables, Figures. Maps, and Related Publications. ISBN 951–690-956–6.
[10] Edraki, M., Golding, S.D., Baublys, K.A., Lawrence, M.G., 2005. Hydrochemistry, mineralogy and sulfur isotope geochemistry of acid mine drainage at the Mt. Morgan mine environment, Queensland, Australia. Appl Geochem 20, 789–805. https://doi.org/10.1016/j.apgeochem.2004.11.004.
[11] Favas, P.J.C., Sarkar, S.K., Rakshit, D., Venkatachalam, P., Prasad, M.N.V., 2016. Acid mine drainages from abandoned mines. Environ Mater Waste 413–462. https://doi.org/10.1016/b978-0-12-803837-6.00017-2.
[12] Galván, L., Olías, M., Cánovas, C.R., Sarmiento, A.M., Nieto, J.M., 2016. Hydrological modeling of a watershed affected by acid mine drainage (Odiel River, SW Spain). Assessment of the pollutant contributing areas. J Hydrol 540, 196–206. https://doi.org/10.1016/j.jhydrol.2016.06.005.
[13] Grande, J.A., de la Torre, M.L., Cerón, J.C., Beltrán, R., Gómez, T., 2010. Overall hydrochemical characterization of the Iberian Pyrite Belt. Main acid mine drainage-generating sources (Huelva, SW Spain). J Hydrol 390, 123–130. https://doi.org/10.1016/j.jhydrol.2010.06.001.
[14] Grande, J.A., Valente, T., De la Torre, M.L., Santisteban, M., Cerón, J.C., Pérez-Ostalé, E., 2014. Characterization of acid mine drainage sources in the Iberian Pyrite Belt: base methodology for quantifying affected areas and for environmental management. Environ Earth Sci 71, 2729. https://doi.org/10.1007/s12665-013-2652-0.
[15] Guerrero, J.L., Gutiérrez-Álvarez, I., Hierro, A., Pérez-Moreno, S.M., Olías, M., Bolívar, J.P., 2021. Seasonal evolution of natural radionuclides in two rivers affected by acid mine drainage and phosphogypsum pollution. Catena 197, 104978. https://doi.org/10.1016/j.catena.2020.104978.
[16] Henderson, G.M., Hall, B.L., Smith, A., Robinson, L.F., 2006. Control on ($^{234}U/^{238}U$) in lake water: a study in the Dry Valleys of Antarctica. Chem Geol 226 (3–4), 298–308. https://doi.org/10.1016/j.chemgeo.2005.09.026.
[17] Hierro, A., Martín, J.E., Olías, M., Vaca, F., Bolívar, J.P., 2013. Uranium behaviour in an estuary polluted by mining and industrial effluents: the Ría of Huelva (SW of Spain). Water Res 47, 6269–6279. https://doi.org/10.1016/j.watres.2013.07.044.
[18] Hierro, A., Olías, M., Ketterer, M.E., Vaca, F., Borrego, J., Cánovas, C.R., Bolívar, J. P., 2014. Geochemical behavior of metals and metalloids in an estuary affected by acid mine drainage (AMD). Environ Sci Pollut R 21, 2611–2627. https://doi.org/10.1007/s11356-013-2189-5.
[19] Hsi, D., Langmuir, D., 1985. Adsorption of uranyl onto ferric oxyhydroxides: application of the surface complexation site-binding model. Geochim Cosmochim Acta 49, 1931–1941. https://doi.org/10.1016/0016-7037(85)90088-2.
[20] IAEA, 2005. Environmental and Source Monitoring for Purposes of Radiation Protection, IAEA Safety Standards Series No. RS-G-1.8, IAEA, Vienna.
[21] IAEA, 2018. Radiation Protection of the Public and the Environment, IAEA Safety Standards Series No. GSG-8, IAEA, Vienna.
[22] Jacobs, J.A., Testa, S.M., Alpers, C.N., Nordstrom, D.K., 2016. An overview of environmental impacts and reclamation efforts at the Iron Mountainmine, Shasta County, California. In: Anderson, R., Ferriz, H. (Eds.), Applied Geology in California. Association of Environmental & Engineering Geologists, pp. 427–446.
[23] Jiao, Y., Zhang, Ch, Su, P., Tang, Y., Huang, Z., Tao, M., 2023. A review of acid mine drainage: formation mechanism, treatment technology, typical engineering cases and resource utilization. Process Saf Environ Prot. https://doi.org/10.1016/j.psep.2022.12.083.
[24] Kim, E., Osseo-Asare, K., 2012. Aqueous stability of thorium and rare earth metals in monazite hydrometallurgy: Eh–pH diagrams for the systems Th–, Ce–, La–, Nd–(PO_4)–(SO_4)–H_2O at 25°C. Hydrometallurgy 113–114, 67–78. https://doi.org/10.1016/j.hydromet.2011.12.007.
[25] Langmuir, D., Herman, J.S., 1980. The mobility of thorium in natural waters at low temperatures. Geochim Cosmochim Acta 44, 1753–1766. https://doi.org/10.1016/0016-7037(80)90226-4.
[26] Leblanc, M., Morales, J.A., Borrego, J., Elbaz-Poulichet, E., 2000. 4500-year-old mining pollution in southwestern Spain: long-term implications for modern mining pollution. Econ Geol 95, 655–662. https://doi.org/10.2113/gsecongeo.95.3.655.
[27] Lei, L., Song, C., Xie, X., Li, Y., Wand, F., 2010. Acid mine drainage and heavy metal contamination in groundwater of metal sulfide mine at arid territory (BS mine, Western Australia). Trans Nonferrous Met Soc China 20, 1488–1493. https://doi.org/10.1016/s1003-6326(09)60326-5.
[28] Lozano, A., Ayora, C., Macías, F., León, R., Gimeno, M.J., Auqué, L., 2020. Geochemical behavior of rare earth elements in acid drainages: modeling achievements and limitations. J Geochem Explor 216, 106577. https://doi.org/10.1016/j.gexplo.2020.106577.
[29] Madejón, P., Caro-Moreno, D., Navarro-Fernández, C.M., Rossini-Oliva, S., Marañón, T., 2021. Rehabilitation of waste rock piles: impact of acid drainage on potential toxicity by trace elements in plants and soil. J Environ Manag 280, 111848. https://doi.org/10.1016/j.jenvman.2020.111848.
[30] Mathuthu, M., Uushona, V., Indongo, V., 2021. Radiological safety of groundwater around a uranium mine in Namibia. Phys Chem Earth Parts A/B/C 122, 102915. https://doi.org/10.1016/j.pce.2020.102915.
[31] McKee, B.A., DeMaster, D.J., Nittrouer, C.A., 1987. Uranium geochemistry on the Amazon shelf: evidence for uranium release from bottom sediments. Geochim Cosmochim Acta 51, 2779–2786. https://doi.org/10.1016/0016-7037(87)90157-8.
[32] Nieto, J.M., Sarmiento, A.M., Olías, M., C_anovas, C.R., Riba, I., Kalman, J., Delvalls, T.A., 2007. Acid mine drainage pollution in the Tinto and Odiel rivers (Iberian Pyrite Belt, SW Spain) and bioavailability of the transported metals to the Huelva estuary. Environ Int 33, 445–455. https://doi.org/10.1016/j.envint.2006.11.010.
[33] Nordstrom, D.K., Wilde, F.D., 1998. Reduction-oxidation potential (electrode method). In: National Field Manual for the Collection of Water Quality Data. US Geological Survey Techniques of Water-resources Investigations. Book 9, Chap. 6.5. https://doi.org/10.3133/twri09A6.5.
[34] Olías, M., Cánovas, C.R., Nieto, J.M., Sarmiento, A.M., 2006. Evaluation of the dissolved contaminant load transported by the Tinto and Odiel rivers (South West Spain). Appl Geochem 21, 1733–1749. https://doi.org/10.1016/j.apgeochem.2006.05.009.
[35] Parkhurst, D.L., Appelo, C.A.J., 2013. Description of input and examples for PHREEQC version 3: computer program for speciation, batch-reaction, one-dimensional transport, and inverse geochemical calculations. U S Geol Surv Tech Methods 6–A43. https://doi.org/10.3133/tm6A43.
[36] Pinedo Vara, I., 1963. Piritas de Huelva. Su historia, minería y aprovechamiento (Ed. Summa, Madrid).
[37] Porcelli, D., Swarzenski, P.W., 2003. The behavior of U- and Th-series nuclides in groundwater. Rev Mineral Geochem 52, 317–361. https://doi.org/10.2113/052031.
[38] Ren, K., Zeng, J., Liang, J., Yuan, D., Jiao, Y., Peng, C., Pan, X., 2021. Impacts of acid mine drainage on karst aquifers: evidence from hydrogeochemistry, stable sulfur and oxygen isotopes. Sci Total Environ, 143223. https://doi.org/10.1016/j.scitotenv.2020.143223.
[39] Riera, J., Cánovas, C.R., Olías, M., 2017. Characterization of main AMD inputs to the odiel river upper reach (SW Spain). Procedia Earth Planet Sci 17, 602–605. https://doi.org/10.1016/j.proeps.2016.12.161.
[40] Sáez, R., Pascual, E., Toscano, M., Almodóvar, G.R., 1999. The Iberian type of volcano– sedimentary massive sulphide deposits. Miner Depos 34, 549–570. https://doi.org/10.1007/s001260050220.
[41] Saïdou, Bochud, F.O., Baechler, S., Moïse, K.N., Merlin, N., Froidevaux, P., 2011. Natural radioactivity measurements and dose calculations to the public: case of the uranium-bearing region of Poli in Cameroon. Radiat Meas 46, 254–260. https://doi.org/10.1016/j.radmeas.2010.11.009.
[42] Saiz, J.L., Ceacero, J.C., 2008. Revegetación de suelos acidificados por minería metálica. Consejería de Medio Ambiente, Junta de Andalucía, Sevilla.
[43] Sánchez-España, J., López-Pamo, E., Santofimia, E., Aduvire, O., Reyes, J., Barettino, D., 2005. Acid mine drainage in the Iberian Pyrite Belt (Odiel river watershed, Huelva, SW Spain): geochemistry, mineralogy and environmental implications. Appl Geochem 20, 1320–1356. https://doi.org/10.1016/j.apgeochem.2005.01.011.
[44] Sánchez-España, J., López Pamo, E., Santofimia Pastor, E., Reyes Andrés, J., Martín Rubí, J.A., 2006. The impact of acid mine drainage on the water quality of the Odiel river (Huelva, Spain): evolution of precipitate mineralogy and aqueous geochemistry along the Concepción-Tintillo segment. Water Air Soil Pollut 173, 121–149. https://doi.org/10.1007/s11270-005-9033-6.
[45] Sánchez-España, J., López Pamo, E., Santofimia Pastor, E., Reyes-Andrés, J., Martín-Rubí, J.A., 2006. The removal of dissolved metals by hydroxysulphate precipitates during oxidation and neutralization of acid mine waters, Iberian Pyrite belt. Aquat Geochem 12, 269–298. https://doi.org/10.1007/s10498-005-6246-7.
[46] Sánchez-España, J., 2007. The behavior of iron and aluminum in acid mine drainage: speciation, mineralogy, and environmental significance. Thermodynamics, Solubility and Environmental Issues. Elsevier,, pp. 137–150. https://doi.org/10.1016/b978-044452707-3/50009-4.
[47] Sarmiento, A.M., Nieto, J.M., Olías, M., Cánovas, C.R., 2009. Hydrochemical characteristics and seasonal influence on the pollution by acid mine drainage in the Odiel River basin (SW Spain). Appl Geochem 24, 697–714. https://doi.org/10.1016/j.apgeochem.2008.12.025.

[48] Serkiz, S.M., Johnson, W.H., 1994. Uranium Geochemistry in Soil and Groundwater at the F and H Seepage Basins. United States. https://doi.org/10.2172/10194263.
[49] Skousen, J.G., Ziemkiewicz, P.F., McDonald, L.M., 2019. Acid mine drainage formation, control and treatment: approaches and strategies. Extr Ind Soc 6, 241–249. https://doi.org/10.1016/j.exis.2018.09.008.
[50] Venkateswarlu, K., Nirola, R., Kuppusamy, S., Thavamani, P., Naidu, R., Megharaj, M., 2016. Abandoned metalliferous mines: ecological impacts and potential approaches for reclamation. Rev Environ Sci Biotechnol 15, 327–354. https://doi.org/10.1007/s11157-016-9398-6.
[51] Villa, M., Manjón, G., Hurtado, S., García-Tenorio, R., 2011. Uranium pollution in an estuary affected by pyrite acid mine drainage and naturally occurring radioactive materials releases. Mar Pollut Bull 62, 269–276. https://doi.org/10.1016/j.marpolbul.2011.04.003.
[52] Wei, C.-L., Lin, S.-Y., Sheu, D.D.-D., Chou, W.-C., Yi, M.-C., Santschi, P.H., Wen, L.-S., 2011. Particle-reactive radionuclides (^{234}Th, ^{210}Pb, ^{210}Po) as tracers for the estimation of export production in the South China Sea. Biogeosciences 8, 3793–3808. https://doi.org/10.5194/bg-8-3793-2011.